Single-Element Needle-Based Ultrasound Imaging of Spine: An *In Vivo* Feasibility Study

Haichong K. Zhang*, Younsu Kim*,
Abhay Moghekar, Nicholas J. Durr, and Emad M. Boctor

The Johns Hopkins University, Baltimore, MD 21218
{hzhang61, ykim99}@jhu.edu, am@jhmi.edu,
ndurr@jhu.edu, eboctor1@jhmi.edu
*equal contribution

Abstract. Spinal interventional procedures such as lumbar puncture require to insert an epidural needle through spine without touching the surrounding bone structures. To minimize the number of insertion trials and insert through a desired direction, an image-guidance technique is necessary. Single-element needle-based ultrasound system is composed of a needle-shaped ultrasound transducer that was mechanically moved to image a spine from skin surface. The needle and imaging direction are inherently registered so that a registration free image guidance is possible. The objective of this study is to show the feasibility of needle-based single-element ultrasound imaging on *in vivo* spine tissue. The experimental validation was performed on a metal wire phantom, ex vivo porcine bone in both water tank and porcine tissue, and spine on living swine model. The needle-shape ultrasound was swept in the lateral direction, and the synthetic aperture focusing was applied to reconstruct B-mode image. The needle-based ultrasound system could visualize the structure, while the reverberation and multi-reflection associated with the needle shaft were observed. These results suggest the potential of the system to be used for in vivo environment.

1 Introduction

Lumbar puncture (LP) is an interventional procedure for collecting cerebrospinal fluid (CSF), which is used to diagnose central nervous system disorders such as encephalitis or meningitis [1]. LP requires inserting a needle into the lower lumbar intervertebral space, and conventional LP is mostly performed without image assistance or guidance. This often results in misdiagnosis or damage to surrounding neurovascular structures [2-6]. Obese patients with thick adipose tissue layer further complicate the procedure, and consequently the rate of overall complications doubles compared to non-obese patients [7-8]. Many image-guided solutions have been proposed to resolve this challenge, and a typical approach is to project needle position into external medical imaging modalities such as ultrasound or CT [9-12]. However, this approach not only increases the cost by introducing bulky systems, but also has a limited tracking accuracy depending on the registration performance. Therefore, a low-cost and registration-free guidance system is in demand.

Here, we propose a simple and direct needle insertion platform, enabling image formation from sweeping a needle with single element ultrasound transducer at the its tip. This needle-embedded ultrasound transducer can not only provide one-dimensional depth information as Chiang et al. reported [13-14], but also visually locate the structures by combining transducer location tracking and a synthetic aperture focusing algorithm [15-17]. This system can minimize the hardware cost for production due to its simplicity, and more importantly does not require registration process as the needle and ultrasound images are co-registered by nature. In the prior study, we built a prototype system which consists of a needle-shape transducer and a mounting holster that tracks the rotational position of the needle [18-19]. While the developed system could image wire and spine phantom inside the water tank, the remaining question was that if the system can provide sufficient contrast from a spine under practical environments, where the spine is covered by muscle and fat tissue layers. Therefore, this paper focuses on the validation of the technique with the presence of realistic tissue layers through both *ex vivo* and *in vivo* experiments.

2 Materials and Methods

2.1 Needle-Based Ultrasound Imaging and Synthetic Aperture Focusing

The proposed needle-based ultrasound imaging system is namely a needle-shape device that functions as an ultrasound transducer. This transducer can transmit and receive ultrasound signals, and collects A-line data. By tracking the position of the needle while applying the motion, a virtual array is formed to build a B-mode image [18]. From the image, the operator can identify the position and angle of needle insertion. Synthetic aperture focusing is the reconstruction step to synthesize coherent sub-aperture information at each position of the needle and to form a final image with higher resolution and contrast. In this paper, the translational motion was applied using the translation stage.

2.2 Experiment Setup

As the imaging system, a needle-shaped ultrasound transducer (ndtXducer, USA) that includes the PZT-5H element on the tip was used. The diameter of the element was 1 mm, and its center frequency is 2.17 MHz with a -6db bandwidth of 0.32 MHz. The electrodes of the element are connected to a coaxial cable with a BNC connector so that the needle could be connected to sampling devices. For ultrasound pulse generation and A-line ultrasound signal sampling, US-WAVE (Lecouer, France) is connected to the element electrodes with a 100 Ohm input impedance. The needle was fixed on a translation stage, and we moved it in 0.5 mm step to form a virtual linear array.

The developed system was tested with a metal rod phantom as well as *ex vivo* and *in vivo* porcine spine. For the *ex vivo* study, the porcine spine was placed inside the water tank to confirm the contrast from the bone without the tissue layer first. Then, a porcine muscle tissue layer with 2-3 cm thickness was placed on the top of spine and imaged. Finally, the spine of a Yorkshire pig was imaged for *in vivo* validation, where the dorsal part of the pig was faced top, and the imaging system was fixed on the translation stage and placed above skin surface. Ultrasound gel and water covered by plastic frame and plastic wrap were used for acoustic coupling. The pig was anesthetized, and the minimal respiratory motion was maintained during the imaging sessions.

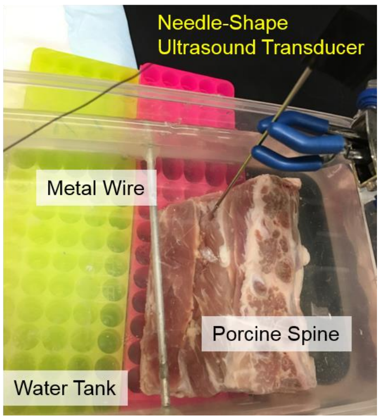

Fig. 1. Experimental setup of phantom and *ex vivo* experiments. The needle-shape ultrasound transducer is held by a gripper which is connected to a translation stage.

3 Results

3.1 Phantom Study

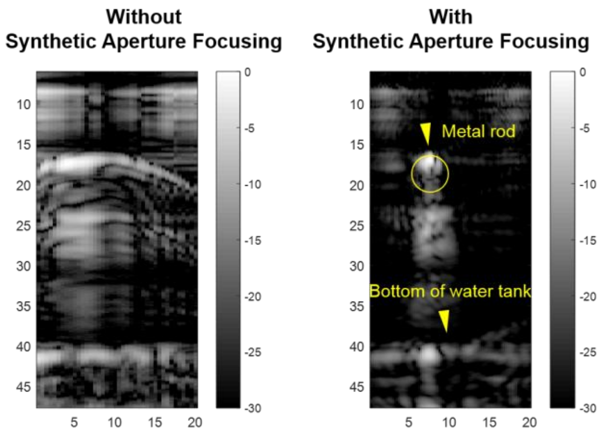

Fig. 2. The needle-based ultrasound images of the metal rod with and without synthetic aperture focusing. The numerical scale is mm.

Figure 2 shows the imaging result of the metal rod phantom. Without synthetic aperture focusing, the metal rod structure was defocused because there is no acoustic focus embedded in the single element transducer. With the synthetic aperture focusing, the metal rod shape appears as its original shape and size although reverberation and multi-reflections are observed beyond the metal rod due to the single-element needle structure. The speed-of-sound was set to 1490 m/s, the aperture size of 40 mm was used in beamforming.

3.2 *Ex Vivo* Demonstration

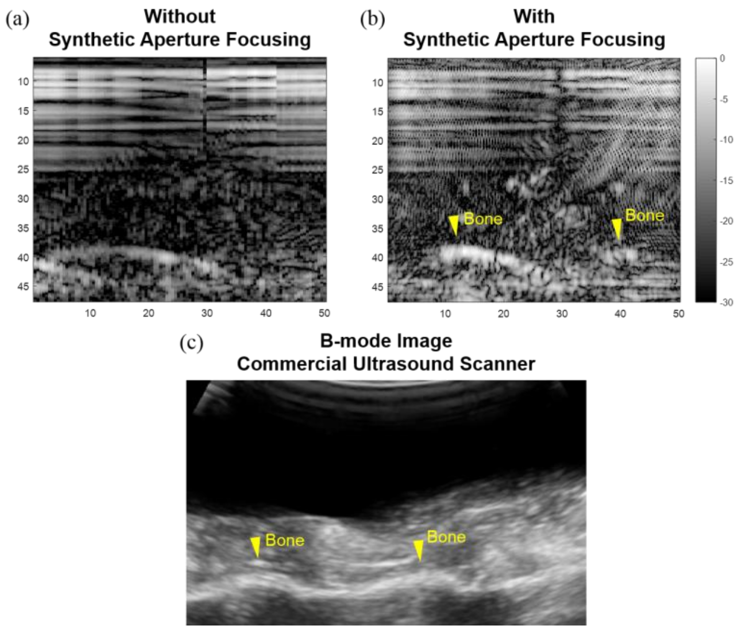

Fig. 3. The needle-based ultrasound images of *ex-vivo* porcine spine placed inside the water tank. (a) Before and (b) after applying synthetic aperture focusing. The numerical scale is mm. (c) The reference image taken at the similar region using a commercial ultrasound scanner.

We tested the visibility of *ex vivo* porcine spine under two conditions. In the first condition, we placed porcine spine bones surrounded by a thin muscle tissue at the bottom of a water tank. A clinical ultrasound scanner (SonixTouch, Ultrasonix, Canada) with a convex probe (C5-2, Ultrasonix, Canada) was used to confirm the bone structure for reference. We collected A-line data at 80 positions by moving in 0.5 mm step in the sagittal plane direction. In Fig. 3, two images are shown for comparison: an image built without synthetic aperture focusing, and the other image with synthetic aperture focusing, where the aperture size of 40 mm was used. Although a bone structure located at the left side of the images was depicted in both images, the other bone located at the right side of the images is clearly visible only in the image with synthetic aperture focusing.

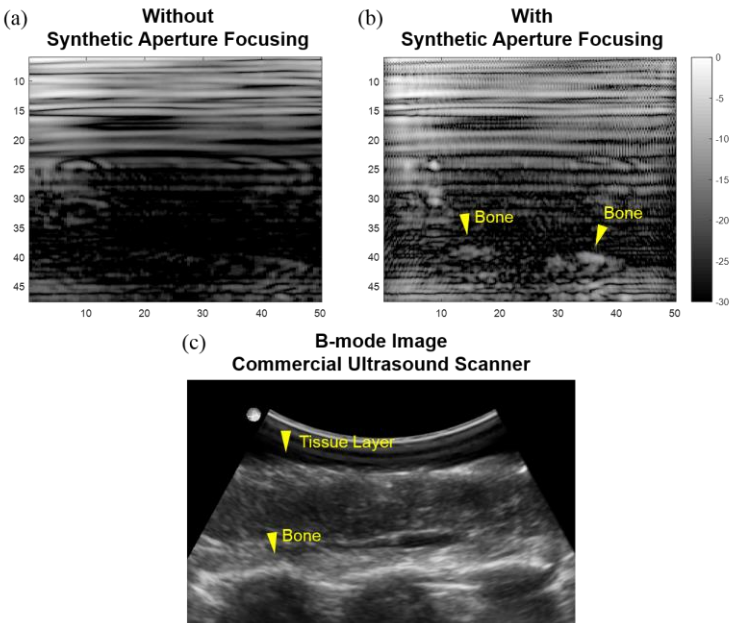

Fig. 4. The needle-based ultrasound images of *ex-vivo* porcine spine placed under the porcine tissue. (a) Before and (b) after applying synthetic aperture focusing. The numerical scale is mm. (c) The reference image taken at the similar region using a commercial ultrasound scanner.

In the second condition, we performed spine bone imaging through porcine muscle tissue to observe the tolerance to a more challenging environment. We stacked a porcine muscle layer on top of the spine bone. The received echo signals were attenuated more compared to the previous *ex vivo* experiment in the water tank. Two bone structures were confirmed in the synthetic aperture focusing image while these structures were barely visible before applying the synthetic aperture focusing.

3.3 *In Vivo* Demonstration

A spine of Yorkshire pig was imaged for *in vivo* validation. We scanned the porcine spine from both sagittal and transverse planes. In both cases, the imaging needle was translated for 40 mm corresponding to 80 positions. We used a commercially available convex probe (C3, Clarius, Canada) for reference. To minimize the effect of motion artifact, the aperture size of 20 mm was used in beamforming. Figures 5 and 6 show the results. For the sagittal view, two spinous processes were captured in the needle-based ultrasound image, and the position of these processes matched with that in the reference image. For the transverse view, it was challenging to confirm the same structure visible in the reference image, but the signal from the processes and facet could be seen in the synthetic aperture focusing image. Nonetheless, the imaging system suffers from the noises caused by respiratory motion, ultrasound reverberations and multi-reflections.

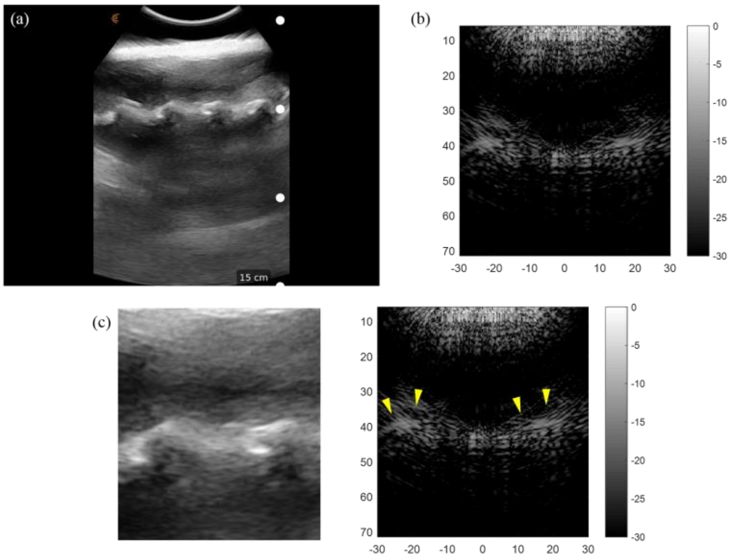

Fig. 5. Experimental results of *in-vivo* porcine spine images in the sagittal plane. (a) The reference image taken using a commercial ultrasound scanner, and (b) the needle-based ultrasound image. The numerical scale is mm. (c) The comparison of the highlighted region of (a) (left) and (b) (right). The yellow arrow indicates the bone structure.

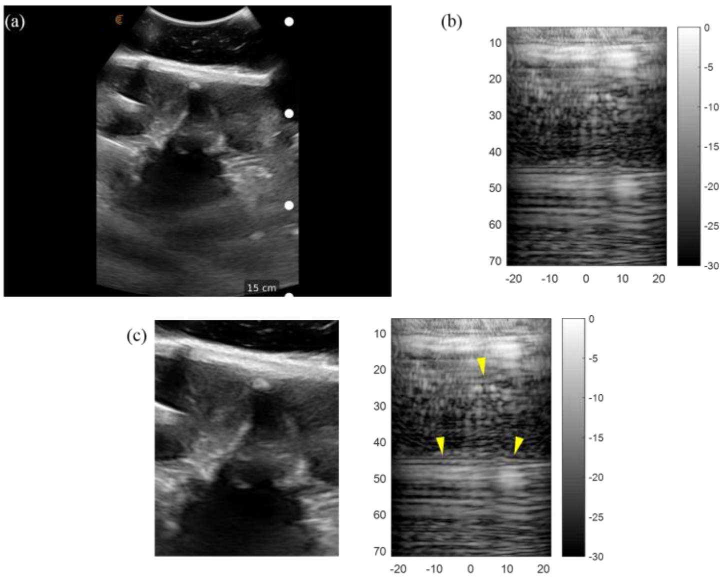

Fig. 6. Experimental results of *in-vivo* porcine spine images in the transverse plane. (a) The reference image taken using a commercial ultrasound scanner, and (b) the needle-based ultrasound image. The numerical scale is mm. (c) The comparison of the highlighted region of (a) (left) and (b) (right). The yellow arrow indicates the bone structure.

4 Discussion and Conclusion

The current standard of care for LP introduces a wide range of iatrogenic complications and places a heavy financial burden on the patient, physician, and healthcare system overall. Our cost-effective single-needle ultrasound system would lead to fewer unnecessary and expensive consequent procedures. Point of care ultrasound technologies need to provide a solution that is built around efficiency within the current workflow. The proposed system accomplishes this by implementing an imaging modality to the current needle itself, providing those important advantages. With addition of the imaging modality, physicians can be trained for LP in a shorter time, without the hassle of keeping track of a separate imaging probe.

In this work, we showed the feasibility of the proposed system under *in vivo* environment and the potential for clinical translation. However, the reconstructed images suffer from artifacts and noises caused by the current needle structure and the sampling device. The image quality can be enhanced by improving the needle fabrication and signal sampling and processing method.

Acknowledgement

The authors would like to acknowledge Mateo Paredes, Karun Kannan, Shayan Roychoudhury for their contributions to the project in a variety of capacities. Financial supports were provided by Johns Hopkins University internal funds, NIH Grant No. R21CA202199, and NIBIB-NIH Grant No. EB015638, and NSF SCH:CAREER Grant No. 1653322. The authors also acknowledge VentureWell, the Coulter Translational Foundation, and the Maryland Innovation Initiative, and the Steven & Alexandra Cohen Foundation for their support throughout this project.

References

1. Køster-Rasmussen, Rasmus, André Korshin, and Christian N. Meyer. "Antibiotic treatment delay and outcome in acute bacterial meningitis," Journal of Infection, 57(6), 449-454. (2008).
2. Armon C., Evans R. W., "Addendum to assessment: prevention of post-lumbar puncture headaches," Neurology 65, 510-512 (2005).
3. American Society for Healthcare Risk Management, "Risk Management Handbook for Health Care Organizations", Jossey-Bass, 5 (2009).
4. Edwards C., Leira E. C., and Gonzalez-Alegre P., "Residency Training: A Failed Lumbar Puncture Is More about Obesity than Lack of Ability," Neurology 84(10), e69-72 (2015).
5. Shah K. H., Richard K. M., et al., "Incidence of traumatic lumbar puncture," Academic Emergency Medicine 10(2), 151-4 (2003).
6. Ahmed S. V., Jayawarna C., and Jude E., "Post lumbar puncture headache: Diagnosis and management," Postgraduate Medical Journal 82(273), 713-716 (2006).
7. Shaikh F., Brzezinski J., Alexander S., Arzola C., Carvalho J. C., Beyene J., and Sung L., "Ultrasound imaging for lumbar punctures and epidural catheterisations: systematic review

and meta-analysis," BMJ 346 (2013).
8. Brook A. D., Burns J., Dauer E., Schoendfeld A. H., and Miller T. S., "Comparison of CT and Fluoroscopic Guidance for Lumbar Puncture in an Obese Population with Prior Failed Unguided Attempt," Journal of NeuroInterventional Surgery 323-27 (2013).
9. Tamas U., Abolmaesumi P., Jalal R., Welch M., Ayukawa I., Nagpal S., Lasso A., Jaeger M., Borschneck D., Fichtinger G., and Mousavi P., "Spinal Needle Navigation by Tracked Ultrasound Snapshots," IEEE Transactions on Biomedical Engineering 59(10), 2766-72 (2012).
10. Moore J., Clarke C., Bainbridge D., Wedlake C., Wiles A., Pace D., and Peters T., "Image Guidance for Spinal Facet Injections Using Tracked Ultrasound," Medical Image Computing and Computer-Assisted Intervention, (2009).
11. Chen E. C. S., Mousavi P., Gill S., Fichtinger G., Abolmaesumi P., "Ultrasound guided spine needle insertion," Proc. SPIE 7625, 762538 (2010).
12. Najafi M., Abolmaesumi P., Rohling R., "Single-Camera Closed-Form Real-Time Needle Tracking for Ultrasound-Guided Needle Insertion," Ultrasound in Medicine and Biology, 41(10), 2663-2676 (2015).
13. Chiang, H. K., et al., "Eyes in the Needle, Novel Epidural Needle with Embedded High-frequency Ultrasound Transducer—Epidural Access in Porcine Model." The Journal of the American Society of Anesthesiologists, 114(6), 1320-1324 (2011).
14. Lee P-Y, Huang C-C, and Chiang H. K., "Implementation of a novel high frequency ultrasound device for guiding epidural anesthesia-in vivo animal study," Proc. IEEE, 2013.
15. Zhang H. K., Lin M., Kim Y., Paredes M., Kannan K. Patel N., Moghekar A., Durr N. J., Boctor E. M., "Toward dynamic lumbar punctures guidance based on single element synthetic tracked aperture ultrasound imaging," Proc. SPIE, 10135, 101350J, 2017.
16. Jensen J. A., Nikolov S. I., Gammelmark K. L., Pedersen M. H., "Synthetic aperture ultrasound imaging," Ultrasonics 44(22), e5-e15 (2006).
17. Zhang H. K., Cheng A., Bottenus N., Guo X., Trahey G. E., Boctor E. M., "Synthetic Tracked Aperture Ultrasound (STRATUS) Imaging: Design, Simulation, and Experimental Evaluation," Journal of Medical Imaging 3(2), 027001 (2016).
18. Zhang, H. K., Kim, Y., et al., "Toward dynamic lumbar puncture guidance using needle-based single-element ultrasound imaging," Journal of Medical Imaging, 5(2), 021224 (2018).
19. Zhang, H. K., Lin, M., Kim, Y., et al., "Toward dynamic lumbar punctures guidance based on single element synthetic tracked aperture ultrasound imaging," Proc. SPIE, 10135, 101350J (2017).